Microsyst Technol (2018) 24:2905–2912
https://doi.org/10.1007/s00542-017-3631-2

TECHNICAL PAPER

Cell therapy using an array of ultrathin hollow microneedles

Florina Silvia Iliescu[1] · Jeremy Choon Meng Teo[2] · Danilo Vrtacnik[3] · Hayden Taylor[4] · Ciprian Iliescu[5,6]

Received: 20 October 2017 / Accepted: 9 November 2017 / Published online: 17 November 2017

Abstract Cell transplantation traditionally employs needles to inject donor cells into tissues to treat certain diseases. However, it is difficult for the current method to achieve multiple parallel equidistant injections, which are ideal for cell therapy. This paper presents a new cell transplantation method using an array of ultrathin microneedles. The main characteristic of the needles is their high aspect ratio: each needle is 500 µm long, and has a 50 µm diameter and a very thin wall (2 µm-thick SiO_2 and 1.5 µm-thick Si_3N_4). An array of such microneedles was successfully used to inject fluorescently labeled Mardin–Darby canine kidney cells into rat liver tissue. Viability of the cells inserted using this method was verified after 5 days. Preliminary results show that this type of microneedle array can be used for cell therapy.

✉ Ciprian Iliescu
ciprian.iliescu@imt.ro; cipi_sil@yahoo.com

1 School of Applied Science, Republic Polytechnic, Singapore, Singapore

2 Department of Biomedical Engineering, Khalifa University of Science and Technology, Abu Dhabi, United Arab Emirates

3 Laboratory of Microsensor Structures and Electronics, Faculty of Electrical Engineering, University of Ljubljana, Trzaska 25, 1000 Ljubljana, Slovenia

4 Department of Mechanical Engineering, University of California, Berkeley, 6159 Etcheverry Hall, Berkeley, CA 94720, USA

5 National Institute for Research and Development in Microtechnologies, IMT-Bucharest, 077190 Bucharest, Romania

6 Academy of Romanian Scientists, Splaiul Independentei Nr. 54, Sector 5, 050094 Bucharest, Romania

1 Introduction

Recent progress in the fabrication of microelectromechanical systems (MEMS) has enabled their application to biomedical devices (BioMEMS), and several of these applications have attained commercial or scientific success. Applications of BioMEMS cover a large spectrum, including biosensors (Roda et al. 2016; Zhou et al. 2016), cell manipulation (Iliescu et al. 2007), tissue engineering (Alhasan et al. 2016; Beißner et al. 2016; Esch et al. 2015), self-assembly of nanomaterials (Iliescu and Tresset 2015; Lu et al. 2016), genomics (Liu et al. 2017), proteomics (Yu et al. 2017), cancer studies (Cima et al. 2013; Lee et al. 2017), drug delivery (Sanjay et al. 2017), and nanoscale imaging (Ni et al. 2017). A well-established example of a biomedical device enabled by microfabrication technology is provided by microneedles, which have been designed for either transdermal or hypodermal delivery of conventional or novel therapeutic agents.

A wide variety of microneedle fabrication processes have been reported, employing a range of materials. Early work on silicon microneedle arrays was reported by Henry et al. (1998) or more recently (Resnik et al. 2015). Silicon microneedles with biodegradable tips have also been reported (Chen et al. 2008). Moreover, 6 mm-long silicon microneedles for localized chemical analysis were reported by Lin and Pisano (1999). More recent research has focused on the fabrication of polymeric biodegradable and/or biocompatible microneedles (Kochhar et al. 2014; Lim et al. 2017; Park et al. 2005). Hollow microneedle arrays have been used in combination with sonophoresis (Chen et al. 2010; Iliescu et al. 2013; Nayak et al. 2016) for transdermal drug delivery. Griss and Stemme reported an exciting microfabrication technique that couples isotropic and anisotropic deep silicon etching to create arrays of out-of-plane microneedles with openings in their sides rather than in their tips (Griss and Stemme 2003). These needles were shown to resist damage and clogging and were proposed for application in transdermal liquid transfer. Meanwhile, arrays of hollow out-of-plane silicon microneedles were presented by Stoeber and Liepmann (2005). However, all these designs are intended to deliver drugs or nanoparticles into the human body, or for chemical analysis. Cell therapy is a potential future application of microneedles fabricated using MEMS techniques, but brings additional requirements for the design of the needles, in part because the shear stresses to which the cells are exposed during injection must be limited to avoid cell damage.

Cell therapies have tremendous potential to treat a wide array of diseases and tissue defects. There are currently three main strategies for cell transplantation. In the first approach, cells are supplied to the organs via the circulatory system (Duffield et al. 2005; Quimby and Dow 2015). In this method, the cells leave the blood vessels and migrate through the capillary endothelia into the target tissue. However, the administration of cells via the organ's blood circulation has its limitations, particularly in cases where the organ to be treated has already suffered damage to its blood circulation system. The second cell transplantation method is to implant into the body an engineered tissue construct that has been prepared, in vitro, using advanced culturing approaches (Ohashi et al. 2007). Engineered tissue implants may consist of one or more layers of cultured cells. The third available method consists of the direct introduction of cell suspensions, which are typically injected into the target tissue (Griffith and Naughton 2002; Lanza et al. 2014). For example, the implantation of cultured myogenic cells into the body is a promising strategy that has been explored for the treatment of myopathies (Skuk and Tremblay 2003). Cell transplantation via direct injection may act by either (a) genetic complementation, or (b) increasing the myogenic pool of muscle fibers (Gojo et al. 2003).

Currently, the most frequently used method to deliver exogenous donor cells to tissues is local intramuscular injection with a single needle (Skuk and Tremblay 2003). However, this method has several disadvantages, most notably the limited and localized fusion of the injected donor cells only at the site of implantation along the injection trajectory. To overcome this limited localized fusion of the injected donor cells, some researchers have made multiple parallel equidistant injections, very close to each other and across the whole tissue to obtain a homogeneous distribution of the donor cells (Skuk and Tremblay 2003). However, manual donor cell injections throughout the whole tissue are extremely time-consuming and lack precision (Skuk and Tremblay 2003). In order to overcome this drawback, we propose a microneedle array to achieve multiple parallel equidistant injections of donor cells into the target tissues.

Here we report the fabrication and testing of a microneedle array for cell transplantation into tissues. With this new design, a series of in vitro tests have been completed in order to assess the cell transplantation. The testing procedure involves staining Mardin–Darby canine kidney (MDCK) cells with fluorescent dye, injecting them into rat liver tissues using the microneedle array, and observing sections of the injected tissue under a fluorescent microscope.

2 Experimental design

2.1 Design of the cell transplantation device

The cell transplantation device consists of a 3D-printed polymeric chamber to carry the donor cell suspension and a silicon die on which the microneedle array is fabricated (Fig. 1). Prior to the injection process, the chamber is connected to the microneedle die. The chamber is then connected to a syringe containing the donor cell suspension.

2.2 Fabrication of the microneedles for the cell transplantation device

The main steps of the fabrication process are presented in Fig. 2. Single-crystal "p"-type silicon wafers, with <100> crystallographic orientation, 1 mm thickness, and a resistivity of 10–25 Ω cm were used. Before processing, the wafers were cleaned in a piranha mixture at 120 °C for

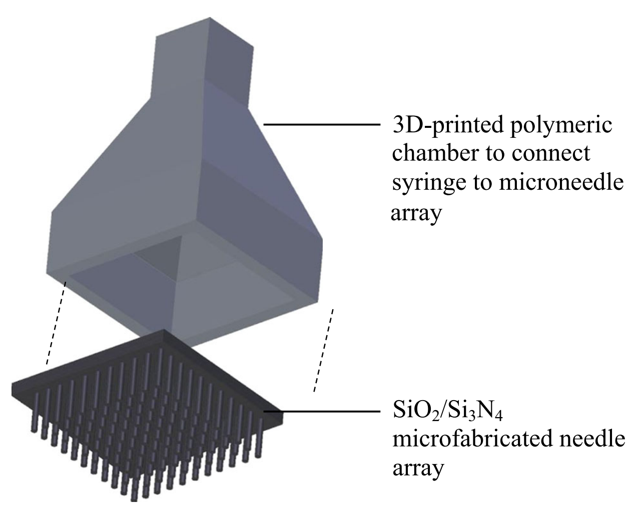

Fig. 1 Concept rendering of the cell transplantation device using a microfabricated SiO_2/Si_3N_4 microneedle array

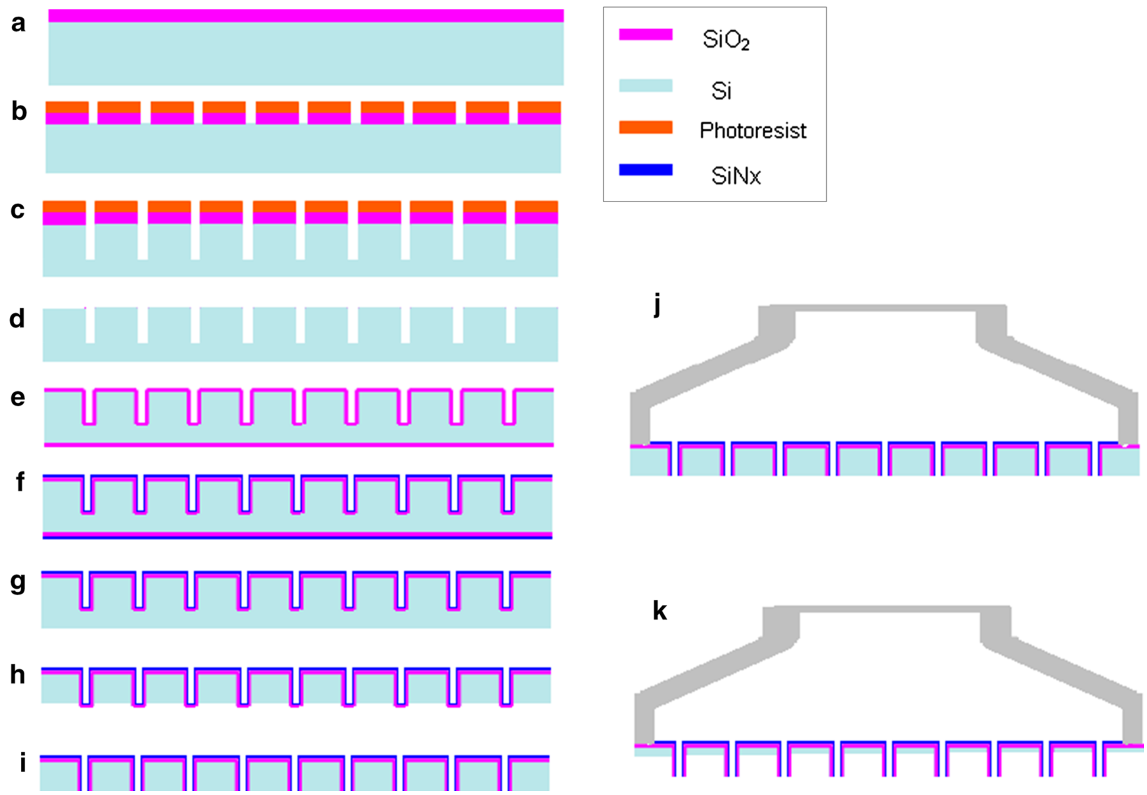

Fig. 2 Process flow of SiO_2/Si_3N_4 microneedles array **a** PECVD SiO_2 layer deposition, **b** patterning of the PECVD SiO_2 layer, **c** etching of 800 µm-deep holes using a Bosch process, **d** removal of the SiO_2/photoresist mask, **e** 2 µm-thick SiO_2 growth in a furnace, **f** 1.5 µm-thick LPCVD Si_3N_4 deposition, **g** removal of the SiO_2/Si_3N_4 layer from the back-side of the wafer, **h** dry etching of silicon (ICP deep RIE), **i** CMP process for removing the top part (SiO_2/Si_3N_4) of the microneedles, followed by dicing of the wafer, **j** assembly of the silicon chip together with the polymer funnel, **k** isotropic release of the needles by dry etching in XeF_2

20 min. A 3 µm-thick SiO_2 layer was deposited on top of the cleaned wafers (Fig. 2a) using a Multiplex Pro-PECVD system (STS) at a temperature of 300 °C, with an applied power of 700 W at 380 kHz, and at a pressure of 900 mTorr. The precursor gases used were SiH_4 and N_2O with flow rates of 51 and 4000 sccm respectively.

The SiO_2 layer was then patterned using a 10 µm-thick photoresist mask (AZ4620 from Clariant: Fig. 2b). The SiO_2 patterning etch was performed in an RIE system using CHF_3 and O_2 (100 and 10 sccm respectively), 2×10^{-2} mbar, a coil power of 1500 W and a plate power of 50 W. The photoresist/SiO_2 mask was then used to etch into the silicon wafer an 8 mm × 8 mm square array of holes on a pitch of 300 µm. The resulting holes were approximately 800 µm deep and 50 µm in diameter. For the silicon etch, a classical Bosch process was used on an ICP deep RIE tool (Adixen AMS101: Fig. 2c). The photoresist mask was removed in 1-methyl-2-pyrrolidon (NMP) resist striper at 70 °C with ultrasonic agitation, while the oxide mask was removed by buffered oxide etching (BOE: Fig. 2d).

A 2 µm-thick SiO_2 layer was then grown by a wet oxidation process in a Tystar furnace (Fig. 2e) at 1050 °C for 12 h. Thermal oxidation, as opposed to PECVD, was selected for this step due to the well-known step coverage of thin films grown in a furnace. The residual stress in the SiO_2 layer was 400 MPa compressive (measured with a KLA-Tencor stress measurement system). In order to compensate the residual stress, a Si_3N_4 layer of thickness 1.5 µm, with a *tensile* residual stress of approximately 400 MPa, was deposited (Fig. 2f) in a Tystar LPCVD furnace at 720 °C for about 14 h, from dichlorosilane (DCS) and NH_3 with flow rates of 25 and 75 sccm respectively.

In the next step (Fig. 2g), the SiO_2/Si_3N_4 layer was removed from the back of the wafer using a dry process in a RIE system (STS) and using the same recipe as for patterning the PECVD SiO_2 mask. A dummy silicon wafer was then bonded with quartz wax (OCON 200, Logitech, with a melting point of 75 °C) to the side of the wafer that was still coated with a SiO_2/Si_3N_4 layer. The bonding was performed in vacuum with 2 h' soaking time at 75 °C in order to dissolve into the wax the air bubbles that were trapped at the interface between the wafers when they were brought into contact. During this process, the applied pressure reduced the thickness of the wax layer to be in the range 7–10 µm.

The bonded wafer assembly was placed into an Adixen AMS 101 deep RIE system and an isotropic dry etching process was used to remove around 200 µm of silicon to expose the tips of the SiO_2/Si_3N_4 microneedles (Fig. 2g). The gases used were SF_6 and C_4F_8 with flow rates of 300 and 150 sccm respectively, the plasma excitation power was 1800 W, and the chuck temperature was − 20 °C.

The tips of the microneedles were opened by chemical–mechanical polishing on a Logitech CDP system using polishing suspension TSF1 from Logitech (Fig. 2i). The dummy wafer was then removed on a hotplate and the residual wax was removed from the process wafer using NMP resist stripper at 80 °C with ultrasonic agitation, followed by piranha cleaning at 120 °C. The wafer was diced on a DISCO DAD3350 dicing saw and the chips were bonded to the polymer connector using optical adhesive NOA63 (Norland; Fig. 2j). After mounting on the plastic connector, in the final step, the microneedles were released by etching the remaining silicon in a XeF_2 etching system that was made in-house. The etching depth was periodically checked using an optical 3D microscope (Keyence).

2.3 Testing the cell transplantation device

To test the transplantation of donor cells, passage 4 Mardin–Darby canine kidney (MDCK) cells, derived from the distal tubule of canine kidney, were employed as a model cell line. These cells were grown in Dulbecco's Modified Eagle Medium (DMEM), supplemented with 5% fetal bovine serum and 500 µL of antibiotic–antimycotic per 50 mL of DMEM. Cells were obtained from American Type Culture Collection, and all components of the cell culture mixture were obtained from Gibco Laboratories, Grand Island, NY, USA. MDCK cells were maintained at 37 °C in 5% CO_2 in air. Prior to cell injection, the membranes of the MDCK cells were labeled with the green-fluorescent stain PKH2GL (Sigma-Aldrich), following the manufacturer's instructions.

The suspension of stained cells (10^6 cells/mL) was drawn into a sterile commercial syringe, which was then connected to the assembled cell transplantation device. Transplantation device was ethanol sterilized and washed thrice with phosphate buffered saline prior to assembly. The microneedle array was inserted into a sample of rat liver tissue and the cells were injected manually and slowly ($\sim$ 1 min) into the tissue. After injection, the microneedle array was left in the tissue for around 30 s and then slowly removed. After the in vitro injection of membrane-labeled MDCK cells into the rat liver tissue, the specimen was placed in a cryosectioning holder, fixed using Tissue-Tek VIP fixative (Sakura Finetek USA, Inc., CA, USA), and placed in a − 20 °C freezer. After fixation, histological cryosections of 10 µm thickness were obtained using a Tissue-Tek Cryo3 Microtome Cryostat (Sakura Finetek USA, Inc., CA, USA). Subsequently, cryosections were viewed with fluorescence microscopy.

3 Results and discussion

3.1 Microneedles in the cell transplantation device

Sets of microneedles with a range of lengths were fabricated for evaluation, by varying the duration of the etching step illustrated in Fig. 2c. The lengths of the newly fabricated sets of microneedles were measured by scanning electron microscopy (SEM) to be 100, 300 and 500 µm. SEM images of the fabricated microneedles are shown in Fig. 3a, b. Figure 3a shows the 500 µm-long microneedles, while Fig. 3b is a top view of a microneedle. Figure 3c is a photograph of a 1 mL syringe attached to the assembled injection chamber, while the injection process is illustrated in Fig. 3d (only 0.1 mL was injected). The connector was fabricated using an Eden350 PolyJet printing system (Stratasys).

3.2 Evaluation of cell viability following the injection process

It is important to evaluate the viability of cells after delivery, to confirm whether they can survive the shear stresses to which they are exposed as they pass through the microneedles. In order to evaluate viability, a $\sim$ 3 mm-thick layer of collagen I hydrogel (Advanced Biomatrix) was deposited into six-well polystyrene plates and cross-linked according to the manufacturer's instructions. Collagen was selected to simulate soft mammalian tissue. For this viability test, injection was carried out with the longest of the microneedles fabricated (500 µm), which are expected to give rise to the largest pressure gradients along the needles and the largest, most challenging shear stresses in the cells. As a separate test, cells were deposited through the needles on to a bare polystyrene tissue culture plate.

Immediately after delivery of the cells to the gel via microinjection, the MDCK cells remained in their rounded trypsinized state, which is similar to that of cells seeded directly on to a tissue culture plate used as a control (Fig. 4a). On the tissue culture plate, cells were dispersed uniformly. In contrast, cells deposited into the gel were localized around the injection positions of the microneedles. The liquid pressure gradients induced by injection caused cells to perfuse along paths of weakness within the gel structure (Fig. 4c).

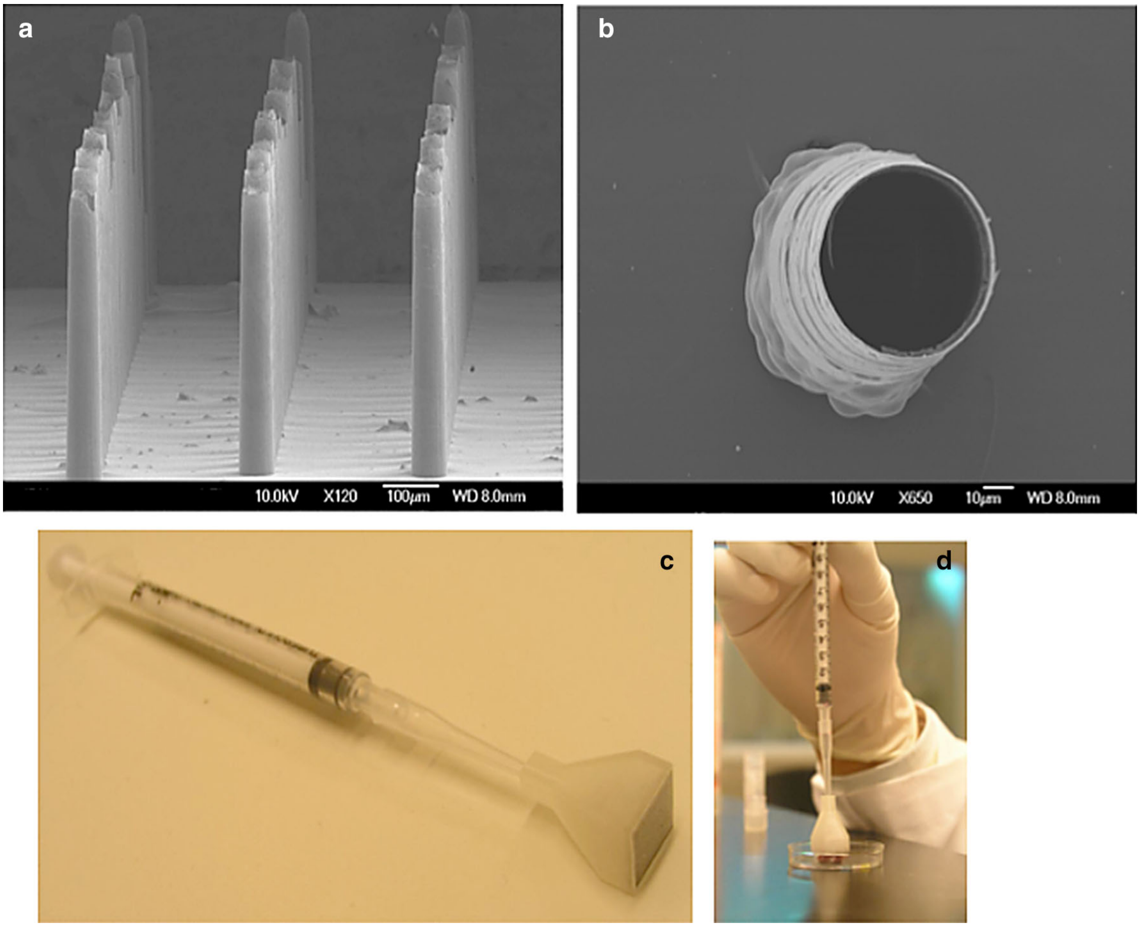

Fig. 3 Images of the fabricated cell injection system. **a** SEM image of an array of 500 µm-long microneedles, **b** top SEM view of a single microneedle, **c** photograph of a syringe attached to the microneedle array via the 3D-printed connector, **d** injection of the cells in the tissue

After 5 days of incubation, cells on the culture plate had proliferated to form a confluent monolayer (Fig. 4b). Cells injected into the gel were still immobilized but had visibly expanded in size and no longer existed in a rounded state (Fig. 4d). This behavior could indicate that the cells were attempting to spread but that the surrounding gel hindered their migration. A live/dead assay showed that the cells in the hydrogel were still viable even though immobilized (Fig. 4e).

A question that can rise is related to the biocompatibility of silica-based materials. Even though the last two decades introduced a large number of studies related to the biocompatibility of these materials (Larrañeta et al. 2016a, b; Ni et al. 2009), the conclusion remains unclear. Although some research questioned their biocompatibility (Kubo et al. 1997), the silicon microneedles became commercially available since 2010 when Micronjet® obtained the FDA approval (Tuan-Mahmood et al. 2013). In our case, the active part/component of the needles (in contact with the tissues) was constructed from SiO_2/Si_3N_4, materials being heavily used in cell culture related applications without cytotoxic effects observed (Tong et al. 2016; Zhang et al. 2011).

3.3 Testing the cell transplantation device

Our in vitro cell transplantation tests employed the microneedle arrays fabricated with different lengths: 100, 300 and 500 µm. These tests showed that during the insertion process, most of the donor cells delivered by 100 and 300 µm microneedles were pushed back by the tissues and few cells were left inside the tissues. This effect could be explained by the small sizes of the cavities created by the short microneedles. It is possible that, after the microneedles were removed, the tissues recovered their original shape and pushed out most of the donor cells. In order to maximize the cell transplantation efficiency, the longest microneedles (500 µm) were therefore employed in the subsequent tests. The results showed the presence of stained cells in the rat liver tissues. This observation meant that by using microneedles, donor cells could be injected into tissue with multiple parallel equidistant injections, and

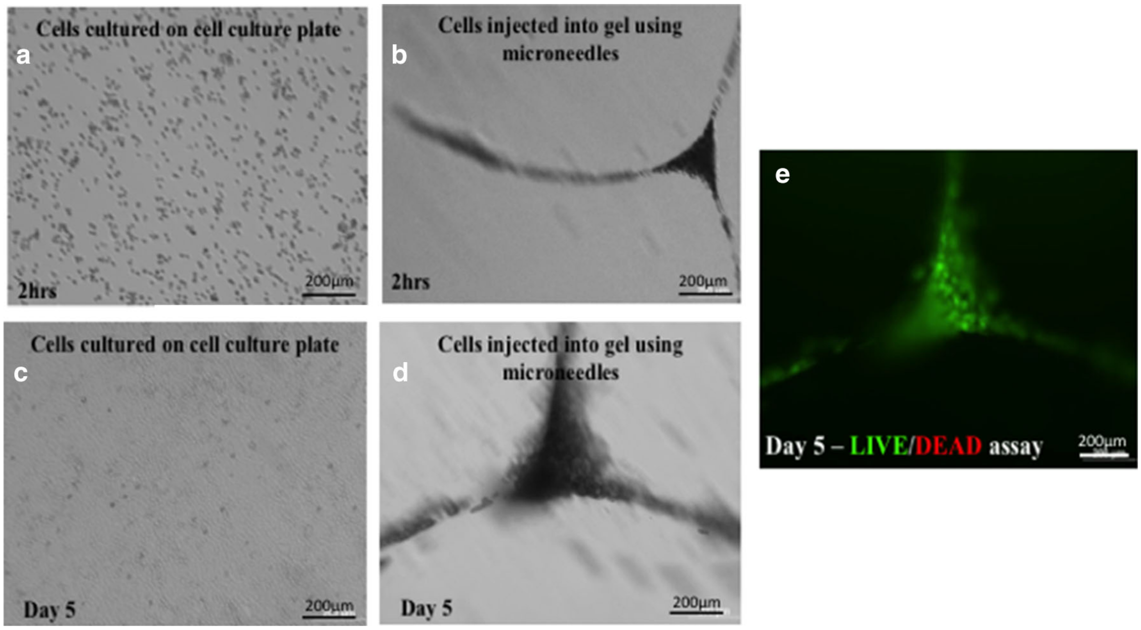

Fig. 4 Testing of the viability of cells after the injection process. **a** MDCK cell culture on a culture plate (after 2 h), **b** MDCK cells injected using microneedles (after 2 h), **c**, **d** MDCK cells on the culture plate and injected in the hydrogel, respectively, after 5 days, **e** live/dead assay of MDCK cells in the hydrogel at day 5

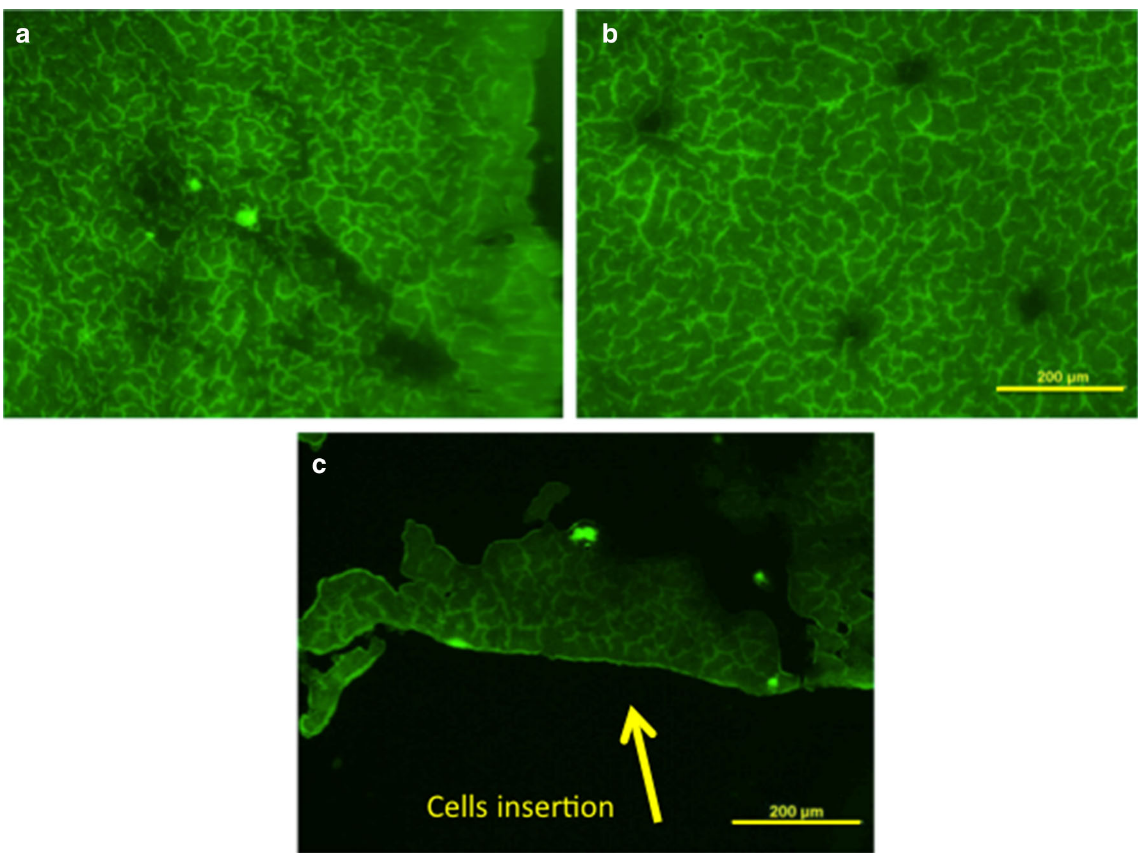

Fig. 5 Images of cell transplantation by using microneedles **a** top view of the tissue, **b** penetration effect of the microneedles, **c** localization of the cells inside the tissue ~ 200 µm deep

in a thin layer near the tissue surface, which is ideal for cell therapies.

The images obtained from fluorescence microscopy are presented in Fig. 5. It should be noted that the cutting direction of histological cryosection shown in Fig. 5b, which is normal to cell injection direction, is different from that shown in Fig. 5a, c. In Fig. 5b, the holes left by the microneedles after insertion can be seen. Figure 5a, c, meanwhile, show that after injection, few cells were transplanted and remained in the tissues, and that the microneedles were able to deliver the donor cells to the tissues successfully. We found also cell on the surface of the tissue (Fig. 5c), due to the pressure generated during insertion, part of the fluid with injected cell is pushed out. The positions of the holes generated by the microneedle array (Fig. 5b) appear uniform due to the soft nature of the tissue and uniformity of the surface.

Compared with microneedles conventionally used in transdermal drug delivery, the needles described here offer considerably higher aspect ratios, having lengths of 500 µm with internal diameters of 47 µm and a wall thickness of approximately 3.5 µm. This geometry allows cell suspensions to be injected readily into tissue. The proposed technique could enable a safe and controlled delivery of cells, which would be of great potential significance for the restoration of functional tissue in parenchymal organs such as kidney and liver. The technique would also allow the homogeneous implantation of cells, for example to position stem cells with angiogenic potential to rebuild a complex and functional capillary system. The main advantage of the proposed method is the uniform distribution of cells in a relatively superficial layer of the tissue. A shallow implantation depth is likely to result in minimal damage to the organ in which the cells are transplanted. Also, the insertion of cells into a superficial layer of the organ reduces the risk of perforating the organ's major blood vessels.

The potential for a desirable delivery profile with little tissue damage is further enhanced by the exceptionally thin needle walls, made from Si_3N_4 to SiO_2. The combination of SiO_2/Si_3N_4 was selected in order to compensate the compressive stress in the thermally grown SiO_2 layer with the tensile stress that characterizes the LPCVD Si_3N_4 layer (Avram et al. 2014; Müller et al. 2001). Moreover, both SiO_2 and Si_3N_4 layers have previously successfully been used as a masking material for isotropic dry etching in XeF_2 (Iliescu et al. 2006, 2011). The use of XeF_2 etching as a dry release method is shown here to be an effective route to producing high-aspect-ratio microneedles with lengths as great as 500 µm and thin walls ($\sim$ 3 µm). Moreover, the hydrophilic nature of the microneedles' surfaces after processing improves the flow of the injected medium containing the cells.

4 Conclusions

In order to deliver a donor cell suspension efficiently to tissue during cell therapy, a novel microfabrication process to produce SiO_2/Si_3N_4 microneedles has been developed and optimized. The reason to use the combination of SiO_2 and Si_3N_4 is to provide microneedles with a hydrophilic surface, thin walls and low stress. By using the optimized microfabrication process, SiO_2/Si_3N_4 microneedles with through-holes have been produced with the following geometry: approximately 500 µm in length, 30–50 µm in diameter and 3–5 µm in wall thickness. The microneedles were bonded to a 3D-printed polymer connector, which was connected in turn to a commercial syringe, to form a cell transplantation device. The cell transplantation device has been tested in vitro by using it to deliver fluorescent-stained MDCK cells to rat liver tissue. Sectional images of the injected tissue show that the MDCK cells have been delivered into the tissue successfully and that a number of cells stayed in the tissues after microneedle removal. From the results, it can be deduced that the microneedles, which are able to achieve the multiple parallel equidistant injections of donor cells into tissues, can be used as components of a promising technique for cell transplantation. Further investigations, especially of the viability and incorporation of donor cells into host tissue, are now needed.

References

Alhasan L, Qi A, Al-Abboodi A, Rezk A, Chan PP, Iliescu C, Yeo LY (2016) Rapid enhancement of cellular spheroid assembly by acoustically driven microcentrifugation. ACS Biomater Sci Eng 2:1013–1022

Avram A et al (2014) Fabrication of thin dielectric membranes for microwave applications. Dig J Nanomater Biostruct 9:475–481

Beißner N, Lorenz T, Reichl S (2016) Organ on chip. In: Microsystems for pharmatechnology. Springer, New York, pp 299–339

Chen B, Wei J, Tay FE, Wong YT, Iliescu C (2008) Silicon microneedle array with biodegradable tips for transdermal drug delivery. Microsyst Technol 14:1015–1019

Chen B, Wei J, Iliescu C (2010) Sonophoretic enhanced microneedles array (SEMA)—improving the efficiency of transdermal drug delivery. Sens Actuators B Chem 145:54–60

Cima I, Wen Yee C, Iliescu FS, Min Phyo W, Hon Lim K, Iliescu C, Han Tan M (2013) Label-free isolation of circulating tumor cells in microfluidic devices: current research and perspectives. Biomicrofluidics 7:011810

Duffield JS, Park KM, Hsiao L-L, Kelley VR, Scadden DT, Ichimura T, Bonventre JV (2005) Restoration of tubular epithelial cells during repair of the postischemic kidney occurs independently of bone marrow-derived stem cells. J Clin Investig 115:1743

Esch EW, Bahinski A, Huh D (2015) Organs-on-chips at the frontiers of drug discovery. Nat Rev Drug Discov 14:248

Gojo S et al (2003) In vivo cardiovasculogenesis by direct injection of isolated adult mesenchymal stem cells. Exp Cell Res 288:51–59

Griffith LG, Naughton G (2002) Tissue engineering—current challenges and expanding opportunities. Science 295:1009–1014

Griss P, Stemme G (2003) Side-opened out-of-plane microneedles for microfluidic transdermal liquid transfer. J Microelectromech Syst 12:296–301

Henry S, McAllister DV, Allen MG, Prausnitz MR (1998) Microfabricated microneedles: a novel approach to transdermal drug delivery. J Pharm Sci 87:922–925

Iliescu C, Tresset G (2015) Microfluidics-driven strategy for size-controlled DNA compaction by slow diffusion through water stream. Chem Mater 27:8193–8197

Iliescu C, Tay FE, Wei J (2006) Low stress PECVD—SiNx layers at high deposition rates using high power and high frequency for MEMS applications. J Micromech Microeng 16:869

Iliescu C, Tresset G, Xu G (2007) Continuous field-flow separation of particle populations in a dielectrophoretic chip with three dimensional electrodes. Appl Phys Lett 90:234104

Iliescu C et al (2011) Residual stress in thin films PECVD depositions. J Optoelectron Adv Mater 13:387–394

Iliescu FS, Sterian AP, Petrescu M (2013) A parallel between transdermal drug delivery and microtechnology. Univ Politech Buchar Sci Bull Ser A Appl Math Phys 75:227–236

Kochhar JS, Anbalagan P, Shelar SB, Neo JK, Iliescu C, Kang L (2014) Direct microneedle array fabrication off a photomask to deliver collagen through skin. Pharm Res 31:1724–1734

Kubo K, Tsukasa N, Uehara M, Izumi Y, Ogino M, Kitano M, Sueda T (1997) Calcium and silicon from bioactive glass concerned with formation of nodules in periodontal-ligament fibroblasts in vitro. J Oral Rehabil 24:70–75

Lanza R, Langer R, Vacanti JP (2014) Principles of tissue engineering, 4th edn. Academic Press, Boston

Larrañeta E, Lutton RE, Woolfson AD, Donnelly RF (2016a) Microneedle arrays as transdermal and intradermal drug delivery systems: materials science, manufacture and commercial development. Mater Sci Eng R Rep 104:1–32

Larrañeta E, McCrudden MTC, Courtenay AJ, Donnelly RF (2016b) Microneedles: a new frontier in nanomedicine delivery. Pharm Res 33:1055–1073. https://doi.org/10.1007/s11095-016-1885-5

Lee W, Tseng P, Di Carlo D (eds) (2017) Microfluidic cell sorting and separation technology. In: Microtechnology for cell manipulation and sorting. Microsystems and Nanosystems. Springer, Cham

Lim SH, Ng JY, Kang L (2017) Three-dimensional printing of a microneedle array on personalized curved surfaces for dual-pronged treatment of trigger finger. Biofabrication 9:015010

Lin L, Pisano AP (1999) Silicon-processed microneedles. J Microelectromech Syst 8:78–84

Liu D, Zhang H, Fontana F, Hirvonen JT, Santos HA (2017) Microfluidic-assisted fabrication of carriers for controlled drug delivery. Lab Chip 17:1856–1883

Lu M, Ozcelik A, Grigsby CL, Zhao Y, Guo F, Leong KW, Huang TJ (2016) Microfluidic hydrodynamic focusing for synthesis of nanomaterials. Nano Today 11:778–792

Müller A et al (2001) Micromachined filters for 38 and 77 GHz supported on thin membranes. J Micromech Microeng 11:301

Nayak A, Babla H, Han T, Das DB (2016) Lidocaine carboxymethylcellulose with gelatine co-polymer hydrogel delivery by combined microneedle and ultrasound. Drug Deliv 23:658–669

Ni M, Tong WH, Choudhury D, Rahim NAA, Iliescu C, Yu H (2009) Cell culture on MEMS platforms: a review. Int J Mol Sci 10:5411–5441

Ni M, Tresset G, Iliescu C (2017) Self-assembled polysulfone nanoparticles using microfluidic chip. Sens Actuators B Chem 252:458–462

Ohashi K et al (2007) Engineering functional two-and three-dimensional liver systems in vivo using hepatic tissue sheets. Nat Med 13:880–886

Park J-H, Allen MG, Prausnitz MR (2005) Biodegradable polymer microneedles: fabrication, mechanics and transdermal drug delivery. J Control Release 104:51–66

Quimby J, Dow S (2015) Novel treatment strategies for feline chronic kidney disease: a critical look at the potential of mesenchymal stem cell therapy. Vet J 204:241–246

Resnik D, Možek M, Pečar B, Dolžan T, Janež A, Urbančič V, Vrtačnik D (2015) Characterization of skin penetration efficacy by Au-coated Si microneedle array electrode. Sens Actuators A 232:299–309

Roda A et al (2016) Progress in chemical luminescence-based biosensors: a critical review. Biosens Bioelectron 76:164–179

Sanjay ST, Zhou W, Dou M, Tavakoli H, Ma L, Xu F, Li X (2017) Recent advances of controlled drug delivery using microfluidic platforms. Adv Drug Deliv Rev (**in press**)

Skuk D, Tremblay JP (2003) Myoblast transplantation: the current status of a potential therapeutic tool for myopathies. J Muscle Res Cell Motil 24:287–302

Stoeber B, Liepmann D (2005) Arrays of hollow out-of-plane microneedles for drug delivery. J Microelectromech Syst 14:472–479

Tong WH et al (2016) Constrained spheroids for prolonged hepatocyte culture. Biomaterials 80:106–120

Tuan-Mahmood T-M, McCrudden MT, Torrisi BM, McAlister E, Garland MJ, Singh TRR, Donnelly RF (2013) Microneedles for intradermal and transdermal drug delivery. Eur J Pharm Sci 50:623–637

Yu F, Zhuo S, Qu Y, Choudhury D, Wang Z, Iliescu C, Yu H (2017) On chip two-photon metabolic imaging for drug toxicity testing. Biomicrofluidics 11:034108

Zhang S et al (2011) A robust high-throughput sandwich cell-based drug screening platform. Biomaterials 32:1229–1241

Zhou Y, Tang L, Zeng G, Zhang C, Zhang Y, Xie X (2016) Current progress in biosensors for heavy metal ions based on DNAzymes/DNA molecules functionalized nanostructures: a review. Sens Actuators B Chem 223:280–294